



Model reduction in model predictive control of combined water quantity and quality in open channels

M. Xu*, P.J. van Overloop, N.C. van de Giesen

Section of Water Resources Management, Faculty of Civil Engineering and Geosciences, Delft University of Technology, Postbox 5048, 2600 GA, Delft, The Netherlands

ARTICLE INFO

Article history:

Received 14 June 2012

Received in revised form

26 November 2012

Accepted 3 December 2012

Available online 18 January 2013

Keywords:

Model predictive control

Open water channel flow

Proper orthogonal decomposition

Water quality control

ABSTRACT

Model predictive control (MPC) is an advanced real-time control technique that uses an internal model to predict the future system behavior and generates optimal control actions by solving an optimization problem. MPC has been more and more applied for controlling open water systems, especially open water channels. Most of the research however focuses on water quantity (water level) control. Since water quality management is recently attracting more attention, extending MPC on combined water quantity and quality management is a logical next step.

In this paper, we study the application of complex models in MPC to control both water quantity and quality. However, because of the online optimization of MPC, the computational time becomes an issue. In order to reduce the computational time, a model reduction technique, Proper Orthogonal Decomposition (POD), is applied to reduce the model order. The method is tested on a Polder flushing case. The results show that POD can significantly reduce the model order for both water quantity and quality with high accuracy. The MPC using the reduced model performs well in controlling combined water quantity and quality in open water channels.

© 2013 Elsevier Ltd. All rights reserved.

1. Introduction

Over the last decades, many control techniques and operation rules have been developed to manage water systems for both water quantity and quality. Most of the research concerns river and reservoir operation. For example, Kerachian and Karamouz (2007), Dhar and Datta (2008), Shirangi et al. (2008) and Chaves and Kojiri (2007) used a Genetic Algorithm (GA) together with water quality simulation models either physically-based or data-driven Neural Network (NN) model, to manage the water quality in river-reservoirs; Mujumdar and Saxena (2004) and Chaves et al. (2004) applied Stochastic Dynamic Programming (SDP) to regulate both water quantity and quality in rivers and reservoirs under uncertainty. These control techniques are intended for mid-term or long-term operation (daily to monthly). One of the intrinsic reasons is that water quality processes are generally characterized by longer time scales compared to water quantity, therefore, it is often difficult to account for water quality when designing a short-term (real-time) controller.

Over the last decades, also many real-time control methods have been developed for short-term water system operation

(minutes to hourly). However, most of the research in this field is on the operation of irrigation and drainage canals and rivers, for example (Schuurmans et al., 1999; van Overloop et al., 2005; Litrico and Fromion, 2005; van Overloop, 2006a; Wahlin and Clemmens, 2006; Negenborn et al., 2010). In these applications, only water quantity is maintained by controlling water levels. In general, water quality is managed through manual operation, for example Dutch polder canals are usually manually operated every couple of days, depending on the system under investigation, in order to flush out the pollution. One of the reasons that combined water quantity and quality management in real-time has not taken off in the past is related to the unavailability of real-time water quality measurements. Real-time control requires continuous measurements within each control step. The traditional laboratory measurement of water quality can not be incorporated in a real-time application. However, real-time water quality control will receive more attention with the development of real-time water quality measurement (Glasgow et al., 2004).

Recently, different real-time control methods have been applied to water quality management in canal systems. For example, Litrico et al. (2011) used an adaptive control method to control canal discharges by adjusting hydraulic structures to restrict algae development. Augustijn et al. (2011) applied dynamic control to prevent salt intrusion in a lake that was modeled as open channel flow. Xu et al. (2010a) applied a model predictive control technique

* Corresponding author. Tel.: +31 0 152782345; fax: +31 0 152785559.
E-mail address: min.xu@tudelft.nl (M. Xu).

to generate an optimal flushing strategy and maintain both water quantity and quality in a polder system.

Real-time control is starting to play an important role in operational water management of open channels. Among different real-time control methods such as Proportional Integral (PI) feedback control and Linear Quadratic Regulator (LQR), Model Predictive Control (MPC) has large advantages in controlling water systems. It uses an internal model to predict the future system behavior over a finite prediction horizon, and generates optimal control actions through optimizing an objective function at every control step. Constraints can also be taken into account in the optimization (Camacho and Bordons, 2004). MPC is completed by a predictive model that provides a prediction of the system's disturbances. Because of the prediction, MPC can take anticipative actions early before undesired changes happen. This research focuses on the application of MPC controlling both water quantity and quality in open channels.

According to the authors' knowledge, Xu et al. (2010a) were first to use MPC to control combined water quantity and quality. They applied simple reservoir models in MPC to maintain water levels and average solute concentrations in a drainage canal. That research showed the possibility of controlling combined water quantity and quality with MPC, however, exposing two drawbacks. First, the internal model for water quality was a reservoir model that assumed complete mixing. Therefore, only the average concentration in the canal reaches could be considered. Second, the research scenario was very simple with water quality change at only one lateral while all the lateral discharges remained unchanged. These two issues of Xu et al. (2010a) were the main trigger for this research. For water quality control in a canal system, more complex and physics-based models are required to capture the

main dynamics. Subsequently, the control targets can be located at the places where water quality needs to be controlled. In addition, it is of importance to analyze the control behavior under more realistic scenarios, for example, with both water quantity and quality changes in all laterals.

MPC solves control problems online, which means that it generates optimal solutions over a finite prediction horizon of which only the first one is implemented in closed-loop. Optimization in MPC requires major computational resources. This requirement restricts the real-time implementation of MPC using models that are accurate but complex. Xu et al. (2010b) applied a model reduction technique, Proper Orthogonal Decomposition (POD), for the Saint-Venant equations to reduce the model order. POD was used to balance control effectiveness with computation time. The research by Xu et al. (2010b) was conducted for water quantity control on a single canal reach without lateral flows. The method looks promising for controlling combined water quantity and quality using complex models with more realistic scenarios in MPC. The control process includes two steps that are illustrated in Fig. 1.

Model reduction, often referred to as model emulation, is a well-established research field. Model emulation is an efficient way of describing the essential natural processes in a system as compact as possible by an emulator with the least possible computational burden. Because of this characteristic it is especially useful for application in optimization routines (Ratto et al., 2012; Razavi et al., 2012). Emulation modeling can be categorized for both static and dynamic models. Ratto et al. (2012) gave intensive literature review on both types. Castelletti et al. (2012a) provided a general framework on both data-based and model-based dynamic emulation modeling, and summarized 6 steps for the emulation procedure. Model emulation is also widely used for sensitivity analysis which

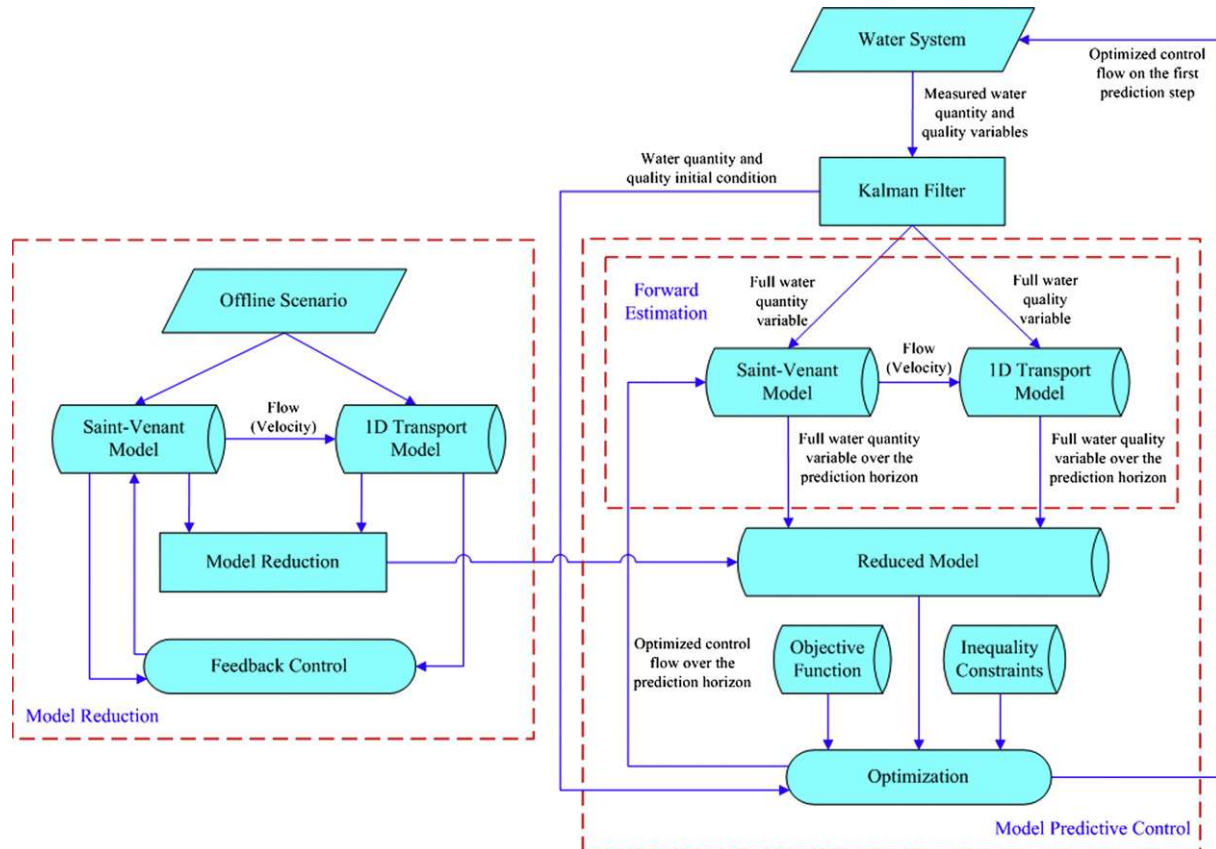


Fig. 1. Work flow of MPC controlling a water system using model reduction technique.

evaluates robustness of complex models, such as (Ratto and Pagano, 2010; Borgonovo et al., 2012).

In this paper, POD model reduction is implemented to generate a reduced model of the combined Saint-Venant equations and general transport equation, based on snapshots of water quantity and quality states taken from an off-line simulation. As such, it is categorized as a model-based dynamic emulation modeling technique. The reduced model can be verified through other scenarios. The reduced model is then used as the internal model in MPC. Hence, the main innovation of this research is to implement complex water quantity and quality models in MPC using a model reduction technique.

MPC algorithms usually cannot be directly implemented without a robustness study. However, there has been intensive research on the robustness of linear and nonlinear MPC algorithms. For example, Pannocchia et al. (2011a) developed a Partial Enumeration MPC, a suboptimal controller, controlling a nonlinear system, and proved the stability of the MPC algorithm. Marruedo et al. (2002), Pannocchia et al. (2011b,c,d) proved the stability and robustness of nonlinear MPC algorithms applying suboptimal solutions to the system under certain assumptions. Given this previous research, it is assumed that applying the MPC algorithm controlling combined water quantity and quality is permitted, although the robustness and stability analysis is not the focus of this research.

The paper is organized as follows. Section 2 introduces a combined water quantity and quality model and its discretization, and describes the method of using POD to generate a reduced model. In Section 3, MPC is introduced to control a water system. It focuses on the formulation of control objectives on combined water quantity and quality, and the state-space model formulation with the reduced model. In Section 4, a Polder flushing case is demonstrated. Section 5 presents the reduced model results and the MPC performance using the reduced model. Section 6 discusses the main issues in controlling combined water quantity and quality. The conclusions are drawn in Section 7.

2. Model reduction on combined open water quantity and quality model

In this section, we describe the combined open water quantity and quality model and the use of Proper Orthogonal Decomposition to reduce the model. The reduced model will be implemented in Model Predictive Control to reduce computation time.

2.1. Combined open water quantity and quality model

The open water quantity and quality model can be described by the Saint-Venant equations and the general transport equation (Chow, 1959; Thomann and Mueller, 1987) as in Eqs. (1)–(3):

$$\frac{\partial A_w}{\partial t} + \frac{\partial Q}{\partial x} = q_l \quad (1)$$

$$\frac{\partial Q}{\partial t} + \frac{\partial(Qv)}{\partial x} + gA_w \frac{\partial \eta}{\partial x} + g \frac{Q|Q|}{C_z^2 \cdot R \cdot A_w} = 0 \quad (2)$$

$$\frac{\partial(A_w c)}{\partial t} + \frac{\partial(Qc)}{\partial x} = \frac{\partial}{\partial x} \left(K A_w \frac{\partial c}{\partial x} \right) + q_l c_l \quad (3)$$

where A_w is the cross sectional area [m^2], Q is the flow [m^3/s], q_l is the lateral flow per unit length [m^2/s], v is the mean velocity [m/s], which equals Q/A_w , η is the water depth above the reference plane [m], C_z is the Chezy coefficient [$m^{1/2}/s$], R is the hydraulic radius [m], which equals A_w/P_f (P_f is the wetted perimeter [m]) and g is the gravity acceleration [m/s^2], K is the dispersion coefficient [m^2/s], c is the

concentration [kg/m^3], c_l is the lateral flow concentration [kg/m^3], t is time [s] and x is horizontal length [m]. Fischer (1979) provides equations to calculate the longitudinal dispersion coefficient K :

$$K = 0.011 \frac{B^2 v^2}{d u_s} \quad (4)$$

where B is the mean width [m], d is the mean water depth [m], $u_s = \sqrt{gRS_b}$ is the shear velocity [m/s], with g the gravitational acceleration ($9.8 m/s^2$), and S_b is the bottom slope of the canal [–].

The discretization of Eqs. (1)–(3) are extensively described in Xu et al. (2010a) and the discretized version can be structured as a linear time-varying state-space model which is commonly used in model-based control techniques, such as Lee et al. (2000) and Falcone et al. (2008). Appendix A provides a detailed description of the discretization and the state-space model formulation. From a control perspective, the general format of the linear time-varying state-space model is as follows:

$$\mathbf{x}^{k+1} = A^k \mathbf{x}^k + B_u^k u^k + B_d^k d^k \quad (5)$$

where A is the system matrix, B_u is the control input matrix, B_d is the disturbance matrix, \mathbf{x} is the state vector that contains water levels and concentrations at discrete points, u is the control input vector that includes the change of control flows, d is the disturbance vector that collects the rest of the terms from the discretization, k is the discrete time step. Using the state-space model formulation, the combined water quantity and quality equations for a canal reach with upstream and downstream hydraulic structures can be written as:

$$\begin{bmatrix} \bar{a}_{1,1} & \bar{a}_{1,2} & 0 & 0 & | & 0 & 0 & 0 & 0 \\ \bar{a}_{2,1} & \bar{a}_{2,2} & \bar{a}_{2,3} & 0 & | & 0 & 0 & 0 & 0 \\ 0 & \ddots & \ddots & 0 & | & 0 & 0 & 0 & 0 \\ 0 & 0 & \bar{a}_{l,l-1} & \bar{a}_{l,l} & | & 0 & 0 & 0 & 0 \end{bmatrix} \begin{bmatrix} e_{\eta,i,1}^{k+1} \\ e_{\eta,i,2}^{k+1} \\ \vdots \\ e_{\eta,i,l}^{k+1} \end{bmatrix} = \begin{bmatrix} \bar{b}_{1,1} & \bar{b}_{1,2} & 0 & 0 \\ \bar{b}_{2,1} & \bar{b}_{2,2} & \bar{b}_{2,3} & 0 \\ 0 & 0 & 0 & 0 \\ 0 & 0 & 0 & 0 \end{bmatrix} \begin{bmatrix} e_{c,i,1}^{k+1} \\ e_{c,i,2}^{k+1} \\ \vdots \\ e_{c,i,l}^{k+1} \end{bmatrix} \\ = I_{2l,2l} \begin{bmatrix} e_{\eta,i,1}^k \\ e_{\eta,i,2}^k \\ \vdots \\ e_{\eta,i,l}^k \end{bmatrix} + \begin{bmatrix} \bar{c}_{1,1} & 0 \\ 0 & 0 \\ \vdots & \vdots \\ 0 & 0 \\ 0 & \bar{c}_{l,2} \end{bmatrix} \begin{bmatrix} Q_{c,1}^{k+1} \\ Q_{c,2}^{k+1} \end{bmatrix} + I_{2l,2l} \begin{bmatrix} d_{\eta,i,1}^k \\ d_{\eta,i,2}^k \\ \vdots \\ d_{\eta,i,l}^k \\ d_{c,i,1}^k \\ d_{c,i,2}^k \\ \vdots \\ d_{c,i,l}^k \end{bmatrix} \quad (6)$$

where i represents the i th canal reach, l is the total number of discrete points of each reach. For example, $e_{\eta,i,l}^k$ and $e_{c,i,l}^k$ are the water level and concentration deviations from their targets at l th discrete point of i th reach at time step k . $Q_{c,1}^k$ and $Q_{c,2}^k$ are the upstream and downstream flows, controlled by the structures, at the reach at time step k . \bar{a} , \bar{b} , \bar{c} and \bar{d} are the time-varying coefficients, d_η and d_c are the water quantity and quality disturbances, respectively. Comparing the

notations in Eq. (6) with the general state-space model notation, it is noticed that: $\mathbf{x}_i^k = [e_{\eta,i,1}^k, \dots, e_{\eta,i,l}^k, e_{c,i,1}^k, \dots, e_{c,i,l}^k]^T$ and $d_i^k = [d_{\eta,i,1}^k, \dots, d_{\eta,i,l}^k, d_{c,i,1}^k, \dots, d_{c,i,l}^k]^T$, however, the control input is the control flow, and we use u_Q for differentiation. Thus, $u_{Q,i}^k = [Q_{c,1}^{k+1}, Q_{c,2}^{k+1}]^T$. Eq. (6) is used to generate the reduced model and the complete model constraints will be formulated in Section 3.2 where the control input vector uses the change of control flow.

The time-varying coefficients (\bar{a} , \bar{b} , \bar{c} and \bar{d}) are known a-priori. They are velocity, water level or concentration related, which change at every time step. The calculation of the time-varying coefficients is referred to ‘forward estimation’, which executes the Saint-Venant and transport model over the prediction. The ‘forward estimation’ uses the optimal control information over the prediction horizon from the previous control step. This can also be considered as model approximation.

The disturbances (d_η and d_c) include physical and virtual disturbances, the latter being necessary to numerically formulate the control problem. Physical disturbances can be uncontrolled lateral discharges and pollution concentrations in this test case. Virtual disturbances are the terms emerging from the discretization of the Saint-Venant equations and the general transport equation. All calculations of the coefficients and variables are formulated in Appendix A. Multiplying the inverse of the first matrix on both sides of Eq. (6) results in a linear time-varying state-space model. Note that considering a linear time-varying (nonlinear) model as a linear model has significant advantages in optimization problems, due to convexity when combined with a quadratic objective function.

2.2. Model reduction on combined water quantity and quality model

Model reduction reduces model order or dimension to decrease computational requirements while maintaining sufficient model accuracy and relevant system dynamics. The idea of model reduction can be tracked back to (Blanning, 1975). Since then, model reduction has been largely adopted in various fields, such as signal analysis, image processing, control engineering, etc (Holmes et al., 1998). Recently, some contributions have appeared in the field of water management, e.g. Siade et al. (2010) and Winton et al. (2011) for groundwater modeling, Ha et al. (2008) for tsunami forecasting and Ravindran (2000) for fluid control.

Model reduction can be either data-driven, building a model by fitting the data through a machine learning process, or model driven, using a mathematical model, to calculate the reduced model (Siade et al., 2010). Recently, Castelletti et al. (2011, 2012b) applied data-driven dynamic emulation modeling for the optimal management of environmental systems. Proper Orthogonal Decomposition (POD) is one of the most popular and widely applied model driven reduction techniques to reduce the model order by calculating basis functions. POD can be applied not only to linear models, but also to nonlinear models, e.g. Hinze and Volkwein (2005) and Chen et al. (2010). The calculation of the basis functions is the key process of POD. Liang et al. (2002) provides an extensive explanation of three POD methods: Karhunen-Loeve Decomposition (KLD), Singular Value Decomposition (SVD), Principal Component Analysis (PCA), and proves the equivalence of these three methods. This paper applies POD with a snapshot method to generate the reduced state-space model for both water quantity and quality.

The snapshot approach has already been applied by several researchers, such as Ravindran (2000), Ha et al. (2007, 2008). The approach takes snapshots of an off-line simulation model and forms a two-point spatial correlation (kernel) matrix. Each snapshot is a column vector containing N states, which are the water

level and concentrations deviations from their targets, in a combined water quantity and quality model. Siade et al. (2010) provides a method to select the optimal snapshot set for a groundwater model. In our research, we try to take as many snapshots as possible from the off-line simulation, in order to cover more flow ranges. For example the range between 1 per 1000 year drought flow and 1 per 1000 year flooding flow. Then the normal scenarios falling in this range can rely on the reduced model generated by such a scenario. On the other hand, the time step of the off-line simulation uses the control time step which is relatively large (in the range of 2 min to 1 h for real-time operation). The full model is executed only once for generating the reduced model. Therefore, taking more snapshots will not significantly increase the computation time.

Sirovich (1987) pointed out that the basis functions are formed by taking the most dominant eigenvectors of the kernel matrix, which are a linear combination of the snapshots:

$$\varphi_i = \sum_{j=1}^M \alpha_j^i \cdot \mathbf{x}_j \quad (7)$$

where φ_i is the i th eigenvector of the kernel matrix, \mathbf{x}_j is the j th state snapshot, M is the number of snapshots, and α_j^i is a coefficient, which is selected from the eigenvector of the correlation matrix CR ($M \times M$ dimension) (Sirovich, 1987):

$$\text{CR}_{ij} = \frac{1}{M} (\mathbf{x}_i^T \cdot \mathbf{x}_j) \quad (8)$$

Finally, the number of the basis functions in use is selected based on the m dominant eigenvalues of the correlation matrix CR, and the combinations of φ_i forms the basis function matrix Φ with a dimension of $N \times m$. Xu et al. (2010b) analyzes the relationship between the reduced model accuracy and the number of reduced states which is selected through trial-and-error method.

Furthermore, snapshots can be taken of disturbances as well, when considering the disturbances as a vector. The same procedure as for the state reduction can be used. Therefore, the original states \mathbf{x}^k and disturbances d^k become a function of the reduced states \mathbf{x}_r^k and reduced disturbances d_r^k , respectively, with respect to the basis function matrix Φ_1 ($N \times m_1$) and Φ_2 ($N \times m_2$):

$$\begin{aligned} \mathbf{x}^k &= \Phi_1 \mathbf{x}_r^k \\ d^k &= \Phi_2 d_r^k \end{aligned} \quad (9)$$

The basis functions are formulated in such a way that the original vector and the projected vector have the least square error (Ha et al., 2008). When Eq. (9) is substituted into the state-space model (5), we obtain:

$$\mathbf{x}_r^{k+1} = A_r^k \mathbf{x}_r^k + B_{u,r}^k u^k + B_{d,r}^k d_r^k \quad (10)$$

where $A_r^k = \Psi_1^T A^k \Phi_1$, $B_{u,r}^k = \Psi_1^T B_u^k$, $B_{d,r}^k = \Psi_1^T B_d^k \Phi_2$, Ψ_1^T is orthogonal with Φ_1 ($\Psi_1^T \Phi_1 = I$), Ψ_2^T is orthogonal with Φ_2 ($\Psi_2^T \Phi_2 = I$), and I is the identity matrix. A_r^k has a dimension of $m_1 \times m_1$, $B_{u,r}^k$ is $m_1 \times n_u$, and $B_{d,r}^k$ is $m_1 \times m_2$. When $m_1 \ll N$ and $m_2 \ll N$, the model order is significantly reduced.

3. Model predictive control of combined water quantity and quality

3.1. Optimization problem formulation

In the combined water quantity and quality control of open channel problems, the most general goal is to keep both the water level and the concentration at the end of a canal reach to their target values, with as few control flow changes as possible. A quadratic

objective function is normally formulated in MPC in order to deal with both positive and negative deviations of the variables (van Overloop, 2006b). An advantage of using a quadratic optimization formulation with a linear model is the guarantee of a convex optimization problem and, thus, a definite global optimum (Leigh, 2004).

Besides these common goals, extra limitations are added to the objective. First, when the water is clean, water quality control should be turned off; Second, when water level is out of the maximum and minimum allowed water level limits, water quantity control dominates and the only objective then becomes bringing the water level back to the water level limit. These two additional goals are achieved by adding soft constraints to the objective function. The soft constraints become active in the objective function when they get out of their bands, which means the penalties are only given for the error outside of the limitation (van Overloop, 2006b). We provide the minimization of the objective function in Eq. (11).

$$\min_{\sum_{s=1}^{n_s} \sum_{j=0}^{n-1} \Delta Q_{c,s}^{k+j}} \left\{ \sum_{i=1}^{n_r} \sum_{j=0}^{n-1} \left(\left(e_{\eta,i,l}^{k+j+1} \right)^T W_{e_{\eta,i}} e_{\eta,i,l}^{k+j+1} + \left(e_{\eta,i,l}^{k+j+1} - e_{\eta,i}^{(k+j+1)*} \right)^T W_{e_{\eta,i,l}-e_{\eta,i}^*} \left(e_{\eta,i,l}^{k+j+1} - e_{\eta,i}^{(k+j+1)*} \right) \right. \right. \\ \left. \left. + \left(e_{c,i,l}^{k+j+1} - e_{c,i}^{(k+j+1)*} \right)^T W_{e_{c,i}} \left(e_{c,i,l}^{k+j+1} - e_{c,i}^{(k+j+1)*} \right) + \left(e_{\eta,i}^{(k+j+1)*} \right)^T W_{e_{\eta,i}^*} e_{\eta,i}^{(k+j+1)*} + \left(e_{c,i}^{(k+j+1)*} \right)^T W_{e_{c,i}^*} e_{c,i}^{(k+j+1)*} \right) \right. \\ \left. + \sum_{s=1}^{n_s} \sum_{j=0}^{n-1} \left[\left(\Delta Q_{c,s}^{k+j} \right)^T W_{\Delta Q_{c,s}} \Delta Q_{c,s}^{k+j} \right] \right\} \quad (11)$$

$$\min_{\sum_{s=1}^{n_s} \sum_{j=0}^{n-1} \Delta Q_{c,s}^{k+j}} \left\{ \sum_{i=1}^{n_r} \sum_{j=0}^{n-1} \left(\left(e_{\eta,r,i,l}^{k+j+1} \right)^T \left(\Phi_1^T W_{e_{\eta,i}} \Phi_1 \right) e_{\eta,r,i,l}^{k+j+1} + \left(e_{\eta,i,l}^{k+j+1} - e_{\eta,i}^{(k+j+1)*} \right)^T W_{e_{\eta,i}^*} \left(e_{\eta,i,l}^{k+j+1} - e_{\eta,i}^{(k+j+1)*} \right) \right. \right. \\ \left. \left. + \left(e_{c,i,l}^{k+j+1} - e_{c,i}^{(k+j+1)*} \right)^T W_{e_{c,i}} \left(e_{c,i,l}^{k+j+1} - e_{c,i}^{(k+j+1)*} \right) + \left(e_{\eta,i}^{(k+j+1)*} \right)^T W_{e_{\eta,i}^*} e_{\eta,i}^{(k+j+1)*} + \left(e_{c,i}^{(k+j+1)*} \right)^T W_{e_{c,i}^*} e_{c,i}^{(k+j+1)*} \right) \right. \\ \left. + \sum_{s=1}^{n_s} \sum_{j=0}^{n-1} \left[\left(\Delta Q_{c,s}^{k+j} \right)^T W_{\Delta Q_{c,s}} \Delta Q_{c,s}^{k+j} \right] \right\} \quad (12)$$

$$\text{s.t. } \begin{cases} x^{k+j+1} = A^{k+j} x^{k+j} + B_u^{k+j} u_Q^{k+j} + B_d^{k+j} d^{k+j} \\ e_{\eta,i,\min} \leq e_{\eta,i,l}^{(k+j+1)*} \leq e_{\eta,i,\max} \\ e_{c,i}^{(k+j+1)*} \leq 0 \\ Q_{c,s,\min} \leq Q_{c,s}^{k+j} \leq Q_{c,s,\max} \end{cases} \quad \begin{pmatrix} j = 0, \dots, n-1 \\ i = 1, \dots, n_r \\ s = 1, \dots, n_s \end{pmatrix}$$

where n_r is the number of canal reach, n_s is the number of controlled structures, n is the prediction horizon, $e_{\eta,i,l}$ is the water level deviation from the target value at the last discretization point of the i th reach, with $W_{e_{\eta,i}}$ as its weighting factor, $e_{\eta,i}^*$ and $e_{c,i}^*$ are the virtual inputs for water level and concentration at the i th reach necessary for the soft constraints, with $W_{e_{\eta,i}^*}$ and $W_{e_{c,i}^*}$ as their weighting factors, respectively, $e_{\eta,i,l} - e_{\eta,i}^*$ and $e_{c,i,l} - e_{c,i}^*$ are the virtual states introduced as soft constraints, with $W_{e_{\eta,i,l}-e_{\eta,i}^*}$ and $W_{e_{c,i,l}-e_{c,i}^*}$ as their weighting factors, $\Delta Q_{c,s}$ is the change of control flow at s th

structure having a weighting factor of $W_{\Delta Q_{c,s}}$. $e_{\eta,i,\min}$ and $e_{\eta,i,\max}$ are the minimum and maximum allowed water level deviations of the i th reach, respectively, $Q_{c,s,\min}$ and $Q_{c,s,\max}$ are the s th minimum and maximum allowed control flows. In the model equality constraints over the prediction horizon, $x^k = [x_1^k, \dots, x_{n_r}^k]^T$, $u_Q^k = [Q_{c,1}^{k+1}, \dots, Q_{c,n_s}^{k+1}]^T$ and $d^k = [d_1^k, \dots, d_{n_r}^k]^T$. Here the disturbance vector d is supposed to be known or can be calculated from a prediction model.

3.2. Optimization problem formulation using reduced model

Because the model used in MPC is the reduced model, the variables in the original objective should be adapted to the reduced states. Therefore, the objective function is changed by substituting the reduced function of Eq. (9) into the objective function:

$$\begin{cases} x_r^{k+j+1} = A_r^{k+j} x_r^{k+j} + B_{u,r}^{k+j} u_r^{k+j} + B_{d,r}^{k+j} d_r^{k+j} \\ \text{s.t. } \begin{cases} e_{\eta,i,\min} \leq e_{\eta,i,l}^{(k+j+1)*} \leq e_{\eta,i,\max} \\ e_{c,i}^{(k+j+1)*} \leq 0 \\ Q_{c,s,\min} \leq Q_{c,s}^{k+j} \leq Q_{c,s,\max} \end{cases} \quad \begin{pmatrix} j = 0, \dots, n-1 \\ i = 1, \dots, n_r \\ s = 1, \dots, n_s \end{pmatrix} \end{cases}$$

where $e_{\eta,r,i,l}^{k+j+1}$ is the reduced water level deviation from the target at the end of the i th reach at j th prediction step of control time step k .

In addition, one of the control objectives is to minimize the number of changes in the flow as little as possible in order to save energy and reduce wear and tear. Therefore, the control flow $Q_{c,s}^{k+j+1}$ in the model is split into $Q_{c,s}^{k+j}$ and $\Delta Q_{c,s}^{k+j+1}$, namely, $Q_{c,s}^{k+j+1} = Q_{c,s}^{k+j} + \Delta Q_{c,s}^{k+j+1}$. The control variable is the change of control flow $\Delta Q_{c,s}^{k+j+1}$ and $Q_{c,s}^{k+j}$ goes into the states. Moreover, according to the control objectives, two soft constraints are

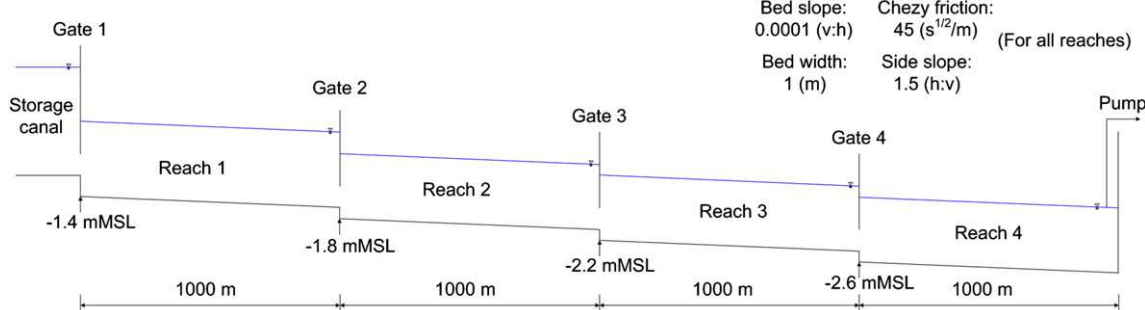


Fig. 2. Schematic view of the test canal.

introduced. Thus, two virtual inputs and states are added to the prediction model. Finally, the time-varying state-space model constraints in MPC become:

shown in Tables 3 and 4 for reduced model generation and verification, and Table 5 for MPC test using the reduced model. For simplicity, a step change in all lateral discharges and concentrations

$$\begin{bmatrix} x_r^{k+j+1} \\ u_Q^{k+j+1} \\ e_{\eta,i,l}^{k+j+1} - e_{\eta,i}^{(k+j+1)*} \\ e_{c,i,l}^{k+j+1} - e_{c,i}^{(k+j+1)*} \end{bmatrix} = \begin{bmatrix} A_r^{k+j} & B_{u,r}^{k+j} & 0 & 0 \\ 0 & 1 & 0 & 0 \\ A_{\eta,i,l}^{k+j} \Phi_1 & B_{u,\eta,i,l}^{k+j} & 0 & 0 \\ A_{c,i,l}^{k+j} \Phi_1 & B_{u,c,i,l}^{k+j} & 0 & 0 \end{bmatrix} \begin{bmatrix} x_r^{k+j} \\ u_Q^{k+j} \\ e_{\eta,i,l}^{k+j} - e_{\eta,i}^{(k+j)*} \\ e_{c,i,l}^{k+j} - e_{c,i}^{(k+j)*} \end{bmatrix} + \begin{bmatrix} B_{u,r}^{k+j} & 0 & 0 \\ 1 & 0 & 0 \\ B_{u,\eta,i,l}^{k+j} & -1 & 0 \\ B_{u,c,i,l}^{k+j} & 0 & -1 \end{bmatrix} \begin{bmatrix} u_{\Delta Q}^{k+j+1} \\ e_{\eta,i}^{(k+j)*} \\ e_{c,i}^{(k+j)*} \end{bmatrix} + \begin{bmatrix} B_{d,r}^{k+j} \\ 0 \\ B_{d,\eta,i,l}^{k+j} \Phi_2 \\ B_{d,c,i,l}^{k+j} \Phi_2 \end{bmatrix} [d_r^{k+j}] \quad (13)$$

where $u_{\Delta Q}^{k+j+1}$ is the vector of change of control flows: $u_{\Delta Q}^{k+j+1} = [\Delta Q_{c,1}^{k+j+1}, \dots, \Delta Q_{c,n_s}^{k+j+1}]^T$. Therefore, the control input vector u^k in Eq. (5) becomes $[(u_{\Delta Q}^{k+1})^T \ e_{\eta,i}^{k*} \ e_{c,i}^{k*}]^T$.

4. Test case

The test canal in this paper is a virtual example of a polder system. It has 4 reaches with 5 structures controlling both water levels and concentrations at the downstream side of each reach. The canal has a trapezoidal cross section. The structures are four gates in series and one pump at the end of the canal. All control structures have a maximum flow capacity of $1.2 \text{ m}^3/\text{s}$. The first gate can introduce clean water from a storage canal with a concentration of 0.4 kg/m^3 . The schematic view is shown in Fig. 2 with geometric parameters. The target values for both water quantity and quality control are listed in Table 1. Each of the reaches is discretized into 100 spatial increments, so there are 800 states in total for both water level and concentration states. The same number applies for the disturbances. It is evident that optimizing such a complex model over 30 prediction steps in this case can presently not be accomplished in an online setting.

Several laterals at each reach flow into the canal with different discharges and concentrations. Their locations are presented in Table 2.

The processes of the experiments include two steps as shown in Fig. 1: 'Model Reduction' block and 'Model Predictive Control' block. Both steps react on certain scenarios of lateral flow changes, as

is assumed for the three scenarios. However, the three step changes are different in magnitude and happen at different time instances and over different durations. In practice, these lateral flow scenarios can be produced by certain rainfall-runoff models.

In the "Model Reduction" block of Fig. 1, a feedback control (Proportional Integral (PI) control) is used in an off-line simulation to maintain the downstream water level and concentration in each reach close to their target values. The most upstream gate is related to the highest concentration among the reaches, and the other structures use upstream control on water levels. The PI control is shown in Eq. (14):

$$\Delta Q_c^k = K_p (e^k - e^{k-1}) + K_i e^k \quad (14)$$

where e^k is the water level or concentration deviation from the target in a reach at time step k , K_p and K_i are the proportional and integral gain factors, which are selected by trial-and-error and shown in Table 6.

A decoupler introduced by (Schuurmans, 1997; Schuurmans et al., 1999) is used between the gates, which adds the downstream gate flow to the upstream gate for each canal reach in order to avoid counteraction disturbances from local controllers between neighboring reaches. The off-line simulation takes 20 h with a simulation time step of 4 min. At each step, a snapshot is taken in this case, thus 300 snapshots in total. With the POD model reduction technique, the model is reduced to 20 states in total (for both water

Table 1
Target values.

Reach	Water quantity target (m)	Water quality target (kg/m^3)
1	-0.4	0.7
2	-0.8	0.7
3	-1.2	0.7
4	-1.6	0.7

Table 2
Locations of laterals in each reach.

Reach	Distance to reach head (m)		
	Lateral 1	Lateral 2	Lateral 3
1	400	800	No third lateral
2	300	700	No third lateral
3	200	500	900
4	500	800	No third lateral

Table 3

Lateral flow scenario for reduced model generation (step changes happen between 8 and 10 h of simulation).

Reach	Lateral 1		Lateral 2		Lateral 3	
	Discharge (m ³ /s)	Concentration (kg/m ³)	Discharge (m ³ /s)	Concentration (kg/m ³)	Discharge (m ³ /s)	Concentration (kg/m ³)
1	0.02 to 0.08	1.0 to 1.6	0.03 to 0.09	1.2 to 1.8	No third lateral	
2	0.02 to 0.08	1.2 to 1.8	0.03 to 0.09	1.4 to 2.0	No third lateral	
3	0.04 to 0.10	0.9 to 1.5	0.02 to 0.08	1.5 to 2.1	0.03 to 0.09	1.8 to 2.4
4	0.02 to 0.08	1.5 to 2.1	0.04 to 0.10	1.0 to 1.6	No third lateral	

Table 4

Lateral flow scenario for reduced model verification (step changes happen between 5 and 8 h of the simulation).

Reach	Lateral 1		Lateral 2		Lateral 3	
	Discharge (m ³ /s)	Concentration (kg/m ³)	Discharge (m ³ /s)	Concentration (kg/m ³)	Discharge (m ³ /s)	Concentration (kg/m ³)
1	0.02 to 0.07	1.0 to 1.5	0.03 to 0.08	1.2 to 1.7	No third lateral	
2	0.02 to 0.07	1.2 to 1.7	0.03 to 0.08	1.4 to 1.9	No third lateral	
3	0.04 to 0.09	0.9 to 1.4	0.02 to 0.07	1.5 to 2.0	0.03 to 0.08	1.8 to 2.3
4	0.02 to 0.07	1.5 to 2.0	0.04 to 0.09	1.0 to 1.5	No third lateral	

Table 5

Lateral flow scenario for testing the reduced model performance (step changes happen between 3 and 6 h of the simulation).

Reach	Lateral 1		Lateral 2		Lateral 3	
	Discharge (m ³ /s)	Concentration (kg/m ³)	Discharge (m ³ /s)	Concentration (kg/m ³)	Discharge (m ³ /s)	Concentration (kg/m ³)
1	0.02 to 0.06	1.0 to 1.4	0.03 to 0.07	1.2 to 1.6	No third lateral	
2	0.02 to 0.06	1.2 to 1.6	0.03 to 0.07	1.4 to 1.8	No third lateral	
3	0.04 to 0.08	0.9 to 1.3	0.02 to 0.06	1.5 to 1.9	0.03 to 0.07	1.8 to 2.2
4	0.02 to 0.06	1.5 to 1.9	0.04 to 0.08	1.0 to 1.4	No third lateral	

levels and concentrations, no controlled release and virtual states) and 30 disturbances. These values are found with trial and error.

The “Water System” in Fig. 1 is represented by the mathematical model in Section 2.1. The test case is simulated for 20 h with a simulation time step of 1 min. In the “Model Predictive Control” block of Fig. 1, the MPC has a control time step of 4 min with a prediction horizon of 2 h. Note that this means that, during the simulation, MPC executes the optimization over 2 h at each 4 min interval and implements only the first control actions, which are kept constant in the simulation for 4 min. In order to distinguish and analyze the interactive and non-interactive effects between water quantity and quality control, the first experiment (Experiment A) turns off the water quality control by setting up the weighting factor on the water quality state to extremely small values. The second experiment (Experiment B) switches on the water quality control and compares the control performance with the first experiment. The weighting factors in MPC are listed in Table 7.

The different control methods are tested in closed-loop on the model of the polder system that acts as real-world. In this off-line setting, it is possible to simulate the Model Predictive Controller that uses the full model, but the simulation time is much larger than real-time.

5. Results

This section presents the reduced model accuracy for both water quantity and quality models, and the results of MPC control performance using the reduced model. In order to demonstrate these

two criteria, the reduced model is compared with the full model. MPC using the reduced model is compared with the MPC using the full model. All the model and control parameters are set the same in the comparisons.

5.1. Reduced model performance

The reduced model is validated with a different lateral scenario and the performance can be analyzed by projecting the reduced model states and disturbances back to the original order as illustrated in Figs. 3 and 4.

Fig. 3 (I and III) shows that the downstream water levels in all reaches are well controlled at their targets with feedback control. The concentration in the last reach is around the target while the concentrations in upstream reaches are always below the targets because of the flushing. Fig. 3 (II and IV) also demonstrates that water levels and concentrations between the reduced model and the original model have a maximum difference in the order of only 10⁻³ m and 10⁻² kg/m³, respectively. This means that the reduced model is representative for the original model and can capture the relevant system dynamics well. The same results occur in the disturbance vector for both water quantity and quality, which has a maximum difference in the order of 10⁻², as shown in Fig. 4 (II and IV). However, each reach has a different model error.

Another way to demonstrate model accuracy is to use the Root Mean Square Error (RMSE), which describes the spread of the reduced model to the original model. Fig. 5 illustrates the RMSE of both water levels and concentrations. The results show a good accuracy of the reduced model on both water quantity and quality, and they are consistent with the model comparisons in Figs. 3 and 4.

5.2. MPC performance under the reduced model

The reduced model can approximate the full dynamic model with a validation scenario according to the results in 5.1. It is

Table 6

Gain factors of the PI control.

	Gate 1	Gate 2	Gate 3	Gate 4	Pump
K_p	4.5	4.5	4.5	4.5	4.5
K_i	0.05	0.45	0.45	0.45	0.45

Table 7

Weighting factors in MPC for all reaches and structures.

Index	1	2	3	4	5
$Q_{e_{n,i}}$	$1/(0.2)^2$	$1/(0.2)^2$	$1/(0.2)^2$	$1/(0.2)^2$	—
$Q_{e_{n,i}}^*$	$1/(1.0 \times 10^{-5})^2$	$1/(1.0 \times 10^{-5})^2$	$1/(1.0 \times 10^{-5})^2$	$1/(1.0 \times 10^{-5})^2$	—
$Q_{e_{ci}} (A)$	$1/(1.0 \times 10^{10})^2$	$1/(1.0 \times 10^{10})^2$	$1/(1.0 \times 10^{10})^2$	$1/(1.0 \times 10^{10})^2$	—
$Q_{e_{ci}} (B)$	$1/(0.2)^2$	$1/(0.2)^2$	$1/(0.2)^2$	$1/(0.2)^2$	—
$R_{e_{n,i}}^*$	$1/(1.0 \times 10^{10})^2$	$1/(1.0 \times 10^{10})^2$	$1/(1.0 \times 10^{10})^2$	$1/(1.0 \times 10^{10})^2$	—
$R_{e_{ci}}^*$	$1/(1.0 \times 10^{10})^2$	$1/(1.0 \times 10^{10})^2$	$1/(1.0 \times 10^{10})^2$	$1/(1.0 \times 10^{10})^2$	—
R_{uj}	$1/(0.02)^2$	$1/(0.02)^2$	$1/(0.02)^2$	$1/(0.02)^2$	$1/(0.02)^2$

'A': the values are used in water quantity control (A); 'B': the values are used in combined water quantity and quality control (B).

expected that MPC will have a good control performance using this reduced model. Figs. 6–9 show the closed-loop MPC performance for both Experiment A and Experiment B in comparison with MPC using the full model. All the figures indicate the advantage of anticipation in MPC using the prediction.

5.2.1. Water quantity control only

In Experiment A, there is only water quantity control. The concentrations are uncontrolled and they are only a consequence of the water quantity control. Fig. 6 shows the controlled water levels

and the subsequent concentrations using both reduced and full models. The controlled water levels in Fig. 6 (I and III) show a decrease in all reaches before 180 min. This is because of the prediction of the increase of lateral discharges, thus pre-releasing occurs. The phenomenon is a result of the control flows in Fig. 7, where the flows of downstream structures increase to release more water, while the flows of upstream structures decrease to introduce less water. In this way, extra space is created in the canal for the coming high flow.

Because each canal reach has a different model error, the influence on the control performance is expected to be different. This

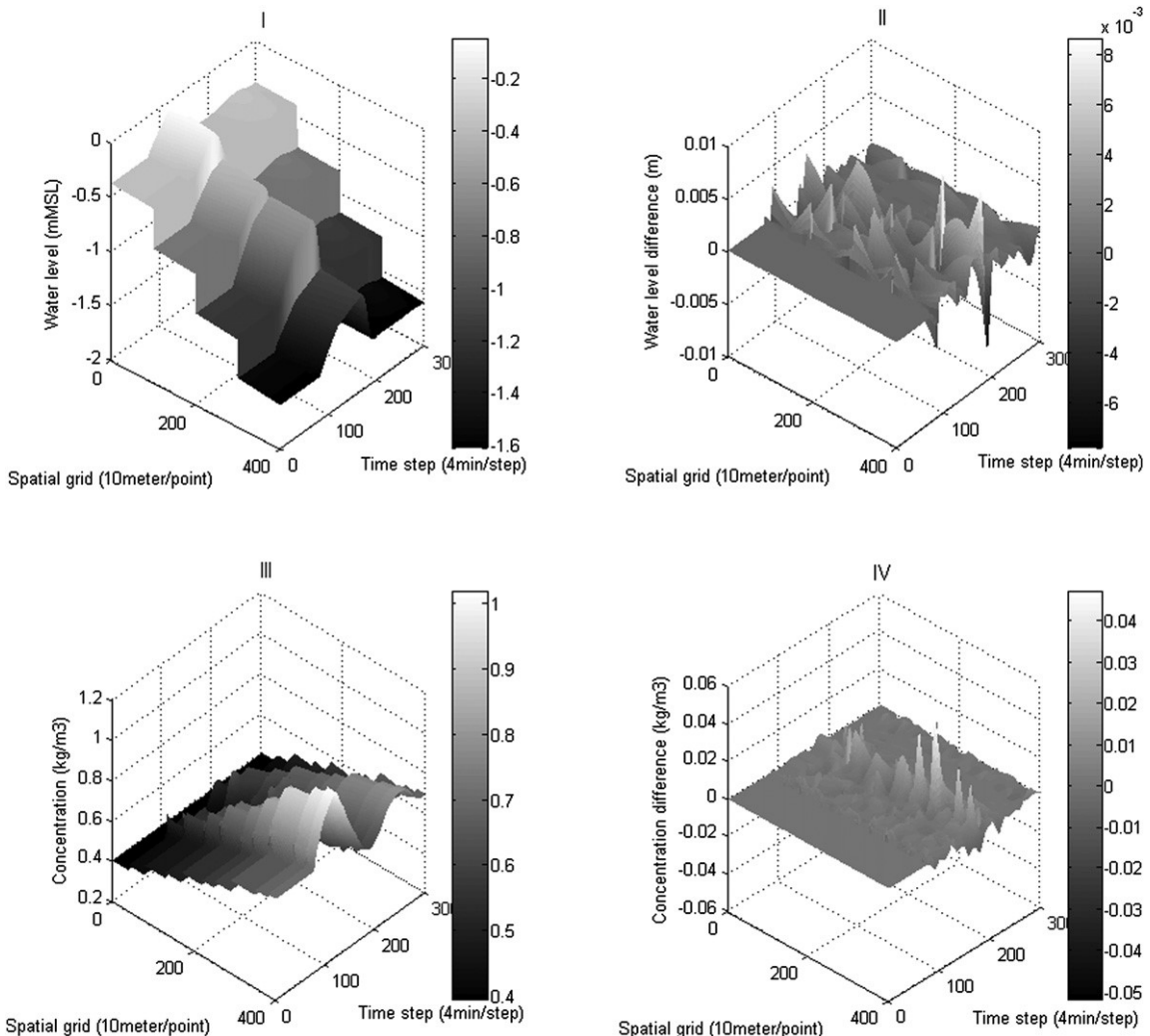


Fig. 3. Reduced water level states (I) and concentration states (III) projected back to the original order, and the water level differences (II) and concentration differences (IV) between the reduced model and the original model.

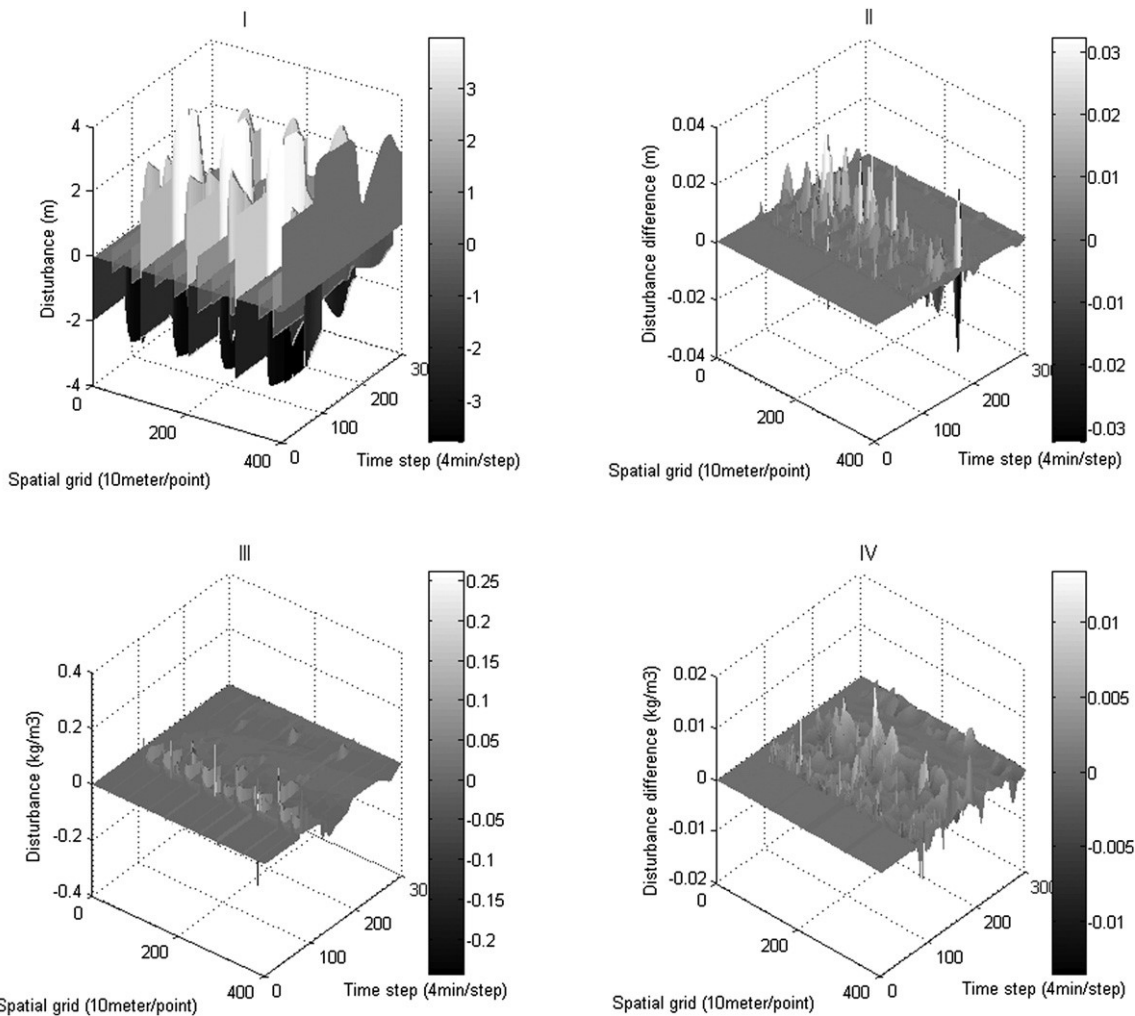


Fig. 4. Reduced water quantity disturbances (I) and quality disturbances (III) projected back to the original order, and the water quantity disturbance differences (II) and water quality disturbance differences (IV) between the reduced model and the original model.

difference is clearly illustrated in Fig. 6, where the water level deviations in (I) are widely spread among the four reaches comparing to (III). However, the water levels are well maintained and the steady-state condition is reached.

5.2.2. Combined water quantity and quality control

In Experiment B, water quality control is added to control both water level and concentration at the downstream end of each reach. Figs. 8 and 9 illustrate the control performance on water

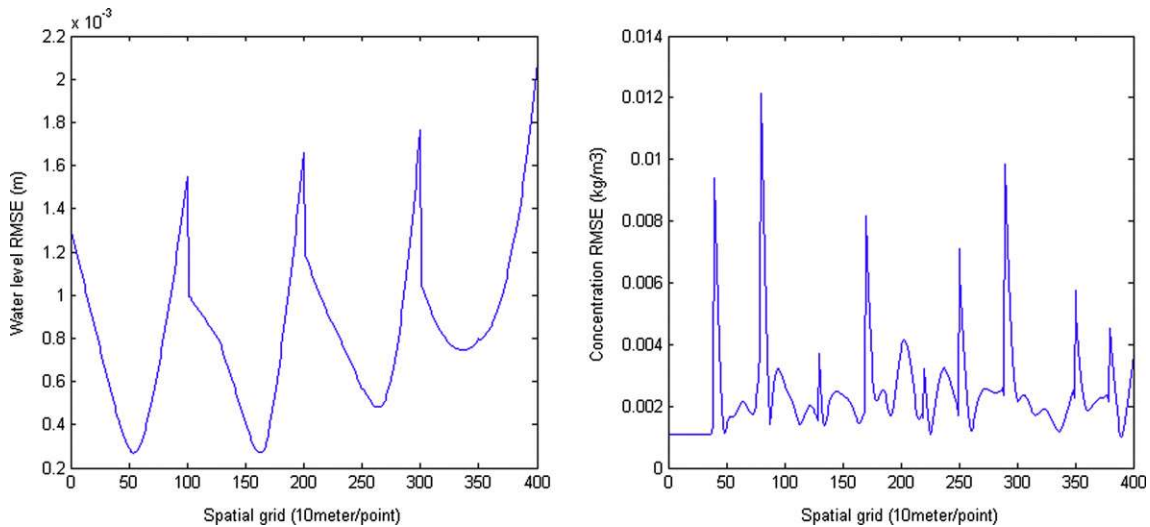


Fig. 5. Root mean square error of the reduced model on water quantity and quality (interpolated scenario).

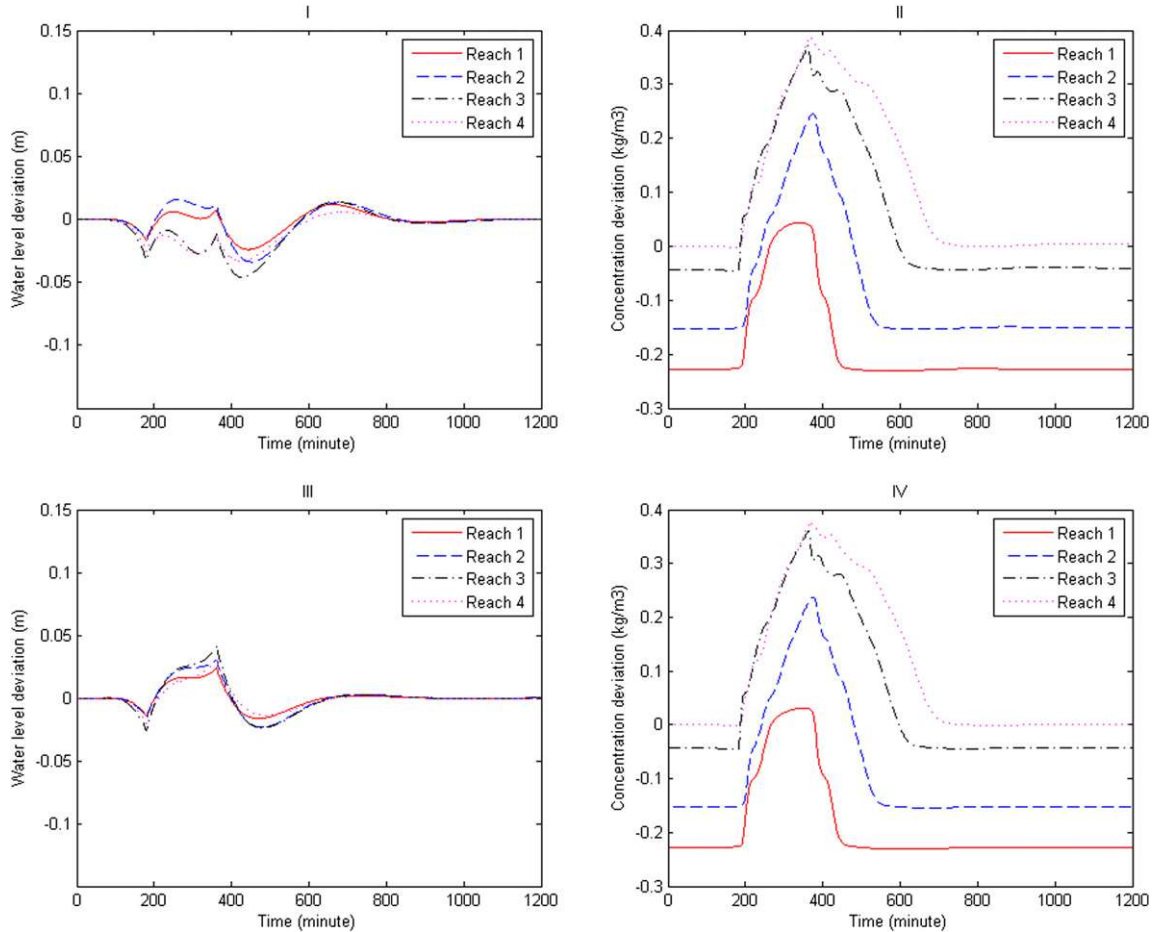


Fig. 6. Controlled water levels (I) and uncontrolled concentrations (II) using the reduced model; controlled water levels (III) and uncontrolled concentrations (IV) using the full model (Experiment A).

level, concentration and control flow. All variables have similar trajectories compared to the water quantity control in Experiment A but show different magnitudes.

The water levels in Fig. 8 (I) also indicate the pre-releasing at the beginning. After pre-releasing, the peak flows come from the laterals with high discharges and concentrations. The upstream gate tries to reduce the discharge in order to let lateral flows raise the

water level to the target. However, this action will deteriorate the water quality and the water quality control requires pumping out more polluted water and introducing clean water. Therefore, the water level drops after rising to a certain level when the water quality control dominates. When water quantity dominates again, the controller tries to raise the water levels. This rotation of control dominance causes the water level fluctuations. After 360 min,

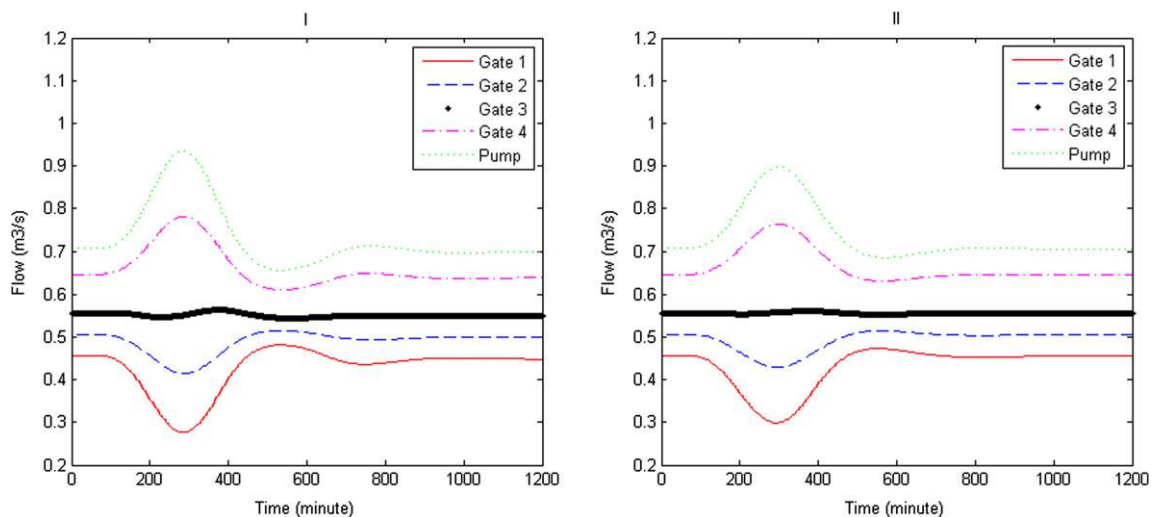


Fig. 7. Control flows (I) using the reduced model and (II) using the full model (Experiment A).

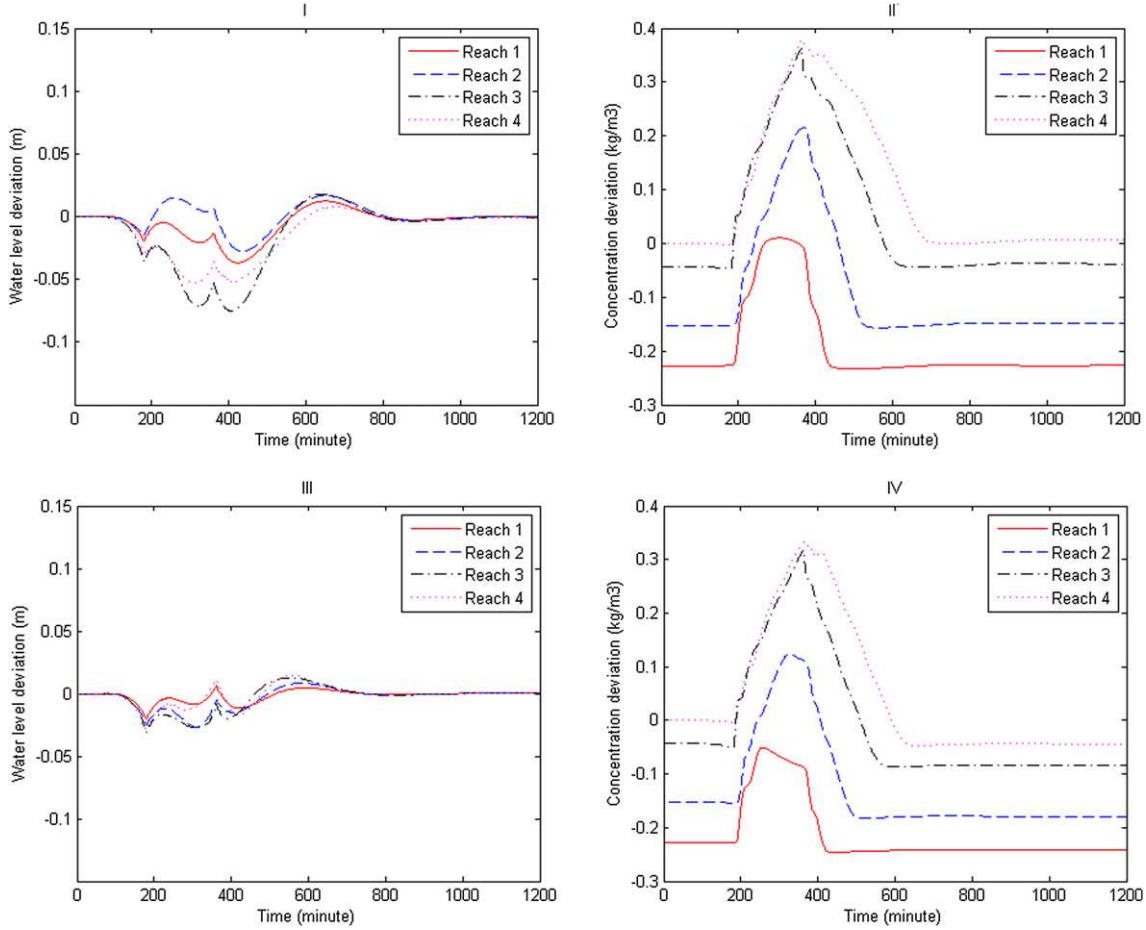


Fig. 8. Controlled water levels (I) and concentrations (II) using the reduced model; controlled water levels (III) and concentrations (IV) using the full model (Experiment B).

when lateral flows are turned back to the original values, the control flows are still relatively high as shown in Fig. 9 and the water levels have a large drop due to the gradual change of the control flows. This is the same phenomenon as found in the results of water quality control. In the end, the system returns back to the targets.

In Fig. 9 (I), the control flows show similar pattern as the water quantity control in Fig. 7 (I), but with larger magnitudes during the

period of lateral flow change. That is because of the added water quality control, which requires releasing more polluted water downstream and introducing more relatively clean water upstream. Because of the large increase of the downstream flows, the upstream flows can not decrease too much due to the water quantity control. These controlled flows introduce more clean water and lead to a relatively low concentration increase, especially in reaches 1 and 2 (comparing Fig. 8 (II) with Fig. 6 (II)). However, because of the large

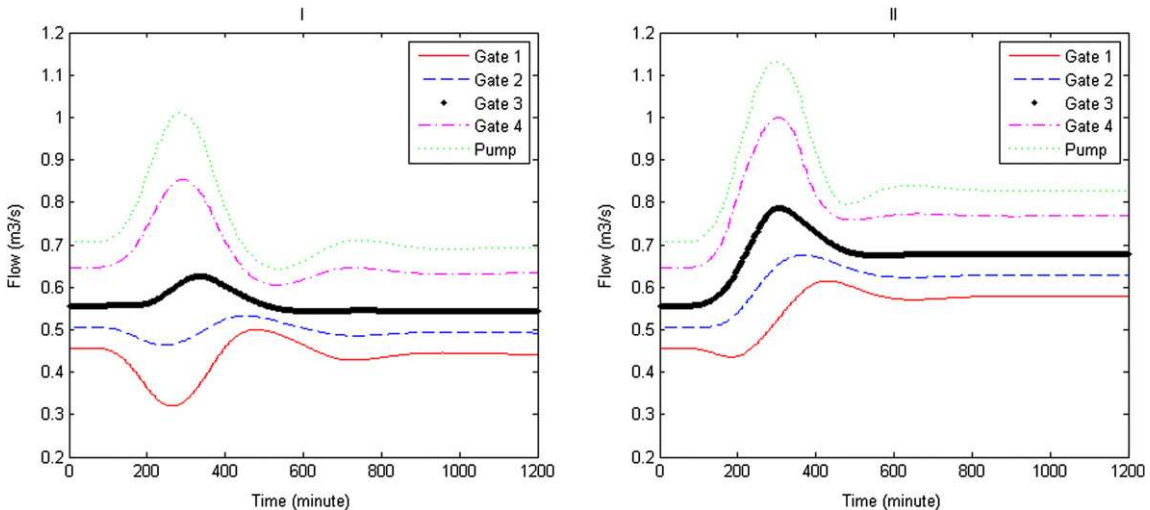


Fig. 9. Control flows (I) using the reduced model and (II) using the full model (Experiment B).

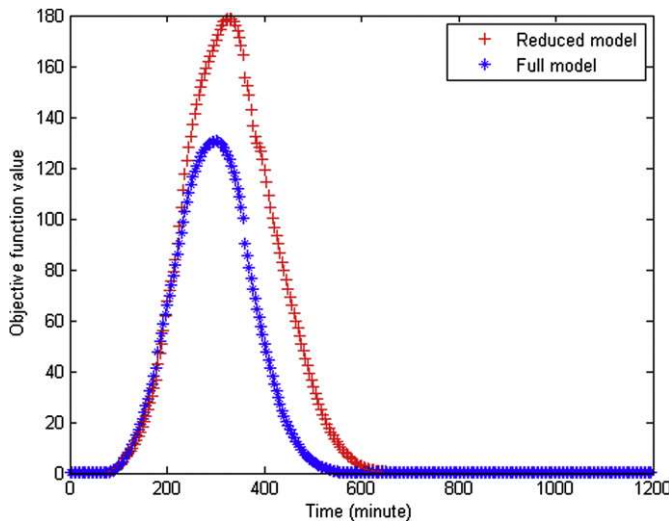


Fig. 10. Objective function value of MPC using reduced and full models.

amount of polluted lateral flow and because the concentration difference among reaches are small, especially in reaches 3 and 4, the magnitude on reducing the concentration peak is limited. On the other hand, the flushing process is faster in combined water quantity and quality control due to the relatively larger flows, and water becomes clean a bit earlier compared to the water quantity Experiment A.

When comparing the MPC results using two different models, we notice that the control flows using the reduced model are smaller compared to those using the full model in Fig. 9, which indicates an underestimation of the states in the reduced model. The high discharges of the full model result in a faster flushing as shown in Fig. 8 (II and IV). Moreover, the water level deviations spread even more widely in Fig. 8 (I) because of the added water quality control, but they are still well controlled.

In Fig. 9, it can be noticed that flow conditions at the end of the control experiments are different. The controlled discharges when using the full model are larger than the initial steady-state conditions and the concentration in the last reach is below the target value, which leads to "over-flushing". However, from a control perspective, the problem is solved properly by MPC using both models. Fig. 10 shows the objective function values of both controllers. After 600 min, both objectives return to zero and the optimization problem is solved. The reason of this "over-flushing" is due to the switch-off of the water quality control when water is clean, while discharge is still too high.

6. Discussion

Water quantity and quality are the two major objectives in this research. They are formulated in a single objective function by assigning different weighting factors to each objective. However, conflicts may easily exist among all the objectives. For example in Experiment B, water quantity control tries to decrease the control flow of the first gate because the lateral inflows will raise the water level. However, from a water quality control point of view, more clean water needs to be introduced into the system, because more polluted lateral inflows will deteriorate the water quality situation. Thus, the first gate flow should increase. The relative importance of water quantity and quality control in the objective function decides the increase or decrease of the control flows.

It can be noticed that the magnitudes of scenarios used for model verification in Table 4 and MPC test in Table 5 are lower than the ones used for reduced model generation in Table 3. This is intended to let the model reduction scenario cover the entire flow

range in the MPC test. In this case, the snapshots taken in the off-line simulation of model reduction can capture the main flow dynamics. Appendix B illustrates a situation where the step change of lateral flows is higher than the one used for the reduced model generation. The results show that the difference between the reduced and original model is around 10 times larger for both state and disturbance vectors, even when the same number of reduced states and disturbances are used. This is due to the flow dynamics that are not captured in the snapshots. Therefore, it is strongly recommended that the model reduction scenario covers the flow and concentration ranges as widely as possible.

This paper demonstrates the possibilities of controlling combined water quantity and quality using a reduced model. In the test case the control locations are selected at the downstream end of each reach. Attention should be paid when the system starts at zero flow and the water is clean and at target. Because water transport takes time, the polluted lateral flow may have already deteriorated the water quality too much before the pollution reaches the downstream side and is detected by the controller. In this case, the average water quality should be considered or the control point/sensor should be located close to the most polluted lateral point.

Because of the differences in scenarios and locations of the control targets, the comparison between this research and Xu et al. (2010a) is only addressed in a qualitative manner. In both cases, the water system can be properly controlled. However, in the present research, more complex water quantity and quality models are applied in MPC using complex scenarios. Thanks to the model reduction, the system can be controlled in real-time. In addition, the location of the control target can be set more flexibly here due to the spatial discretization.

7. Conclusions and future research

This paper studies combined water quantity and quality control and provides a model reduction technique to implement complex high order models in Model Predictive Control. The research demonstrates that the extension of MPC to control both water quantity and quality control using complex models is possible.

According to the comparison between the two experiments, water quantity and quality control may conflict. However, the optimization in MPC can deal with the conflicts and finds the optimal solutions for all objectives. Thanks to the prediction of the flow dynamics in MPC, the water system can respond to the known water quantity and quality disturbances in advance and create extra space for the upcoming problems.

Proper Orthogonal Decomposition is an efficient model reduction method to reduce the model order for both water quantity and quality. From a state-space model perspective, the number of states and disturbances can be significantly reduced while maintaining high accuracy. Because the reduced model can capture the main flow structure, it can be used as the prediction model in MPC to reduce the computational time. With model reduction, MPC could be run in real-time, whereas this was not possible with the full model.

According to the discussion above, some future research can be performed. 1) The computation of Pareto fronts can be useful, in order to assess the trade-off between water quantity and quality objectives. 2) In reality, there are significant uncertainties in both data (lateral scenarios) and prediction models used. It is worth to incorporate uncertainty analysis of real-world applications and the adoption of robust MPC. 3) From an organization point of view, it could be also interesting to split the optimization in two agents, responsible for either water quantity or water quality management at different locations. Instead solving the central problem at once, the two agents need to collaborate in a distributed model predictive control configuration to come to a global optimum.

Appendix A. Combined water quantity and quality state-space model formulation

The one dimensional water quantity and quality model is generally described by the Saint–Venant equations and the general transport equation:

$$\frac{\partial A_w}{\partial t} + \frac{\partial Q}{\partial x} = q_1$$

$$\frac{\partial Q}{\partial t} + \frac{\partial(Qv)}{\partial x} + gA_w \frac{\partial \eta}{\partial x} + g \frac{Q|Q|}{C_z^2 \cdot R \cdot A_w} = 0$$

$$\frac{\partial(A_w c)}{\partial t} + \frac{\partial(Qc)}{\partial x} = \frac{\partial}{\partial x} \left(K A_w \frac{\partial c}{\partial x} \right) + q_1 c_1$$

According to Stelling and Duinmeijer (2003) and Xu et al. (2010a,b), the equations for both water quantity and quality can be spatially discretized with staggered grids. A semi-implicit scheme is applied to the time integration for the Saint–Venant equations, where the advection term in the momentum equation is explicitly discretized by first-order upwinding. The friction term is linearized by setting $|Q|$ to explicit. The remaining terms use the implicit scheme. The time integration for the transport model is fully implicit. The water quantity and quality equations are solved through a tri-diagonal format:

$$\begin{bmatrix} \bar{a}_{1,1} & \bar{a}_{1,2} & 0 & 0 & | & 0 & 0 & 0 & 0 \\ \bar{a}_{2,1} & \bar{a}_{2,2} & \bar{a}_{2,3} & 0 & | & 0 & 0 & 0 & 0 \\ 0 & \ddots & \ddots & 0 & | & 0 & 0 & 0 & 0 \\ 0 & 0 & \bar{a}_{l,l-1} & \bar{a}_{l,l} & | & 0 & 0 & 0 & 0 \\ \hline 0 & 0 & 0 & 0 & | & \bar{b}_{1,1} & \bar{b}_{1,2} & 0 & 0 \\ 0 & 0 & 0 & 0 & | & \bar{b}_{2,1} & \bar{b}_{2,2} & \bar{b}_{2,3} & 0 \\ 0 & 0 & 0 & 0 & | & 0 & \ddots & \ddots & 0 \\ 0 & 0 & 0 & 0 & | & 0 & 0 & \bar{b}_{l,l-1} & \bar{b}_{l,l} \end{bmatrix} \begin{bmatrix} e_{\eta,i,1}^{k+1} \\ e_{\eta,i,2}^{k+1} \\ \vdots \\ e_{\eta,i,l}^{k+1} \\ \hline e_{c,i,1}^{k+1} \\ e_{c,i,2}^{k+1} \\ \vdots \\ e_{c,i,l}^{k+1} \end{bmatrix}$$

$$\bar{a}_{i,i-1} = -\frac{\Delta t}{\Delta x T_{w,i}^k} A_{w,i-1}^k f u_{i-1/2}^k,$$

$$\bar{a}_{i,i} = 1 + \frac{\Delta t}{\Delta x T_{w,i}^k} \left(A_{w,i-1}^k f u_{i-1/2}^k + A_{w,i}^k f u_{i+1/2}^k \right)$$

$$\bar{a}_{i,i+1} = -\frac{\Delta t}{\Delta x T_{w,i}^k} A_{w,i}^k f u_{i+1/2}^k,$$

$$\bar{b}_{i,i-1} = -\frac{\Delta t}{\Delta x A_{w,i}^k} \frac{K_{i-1}^{k+1} \bar{A}_{w,i-1/2}^{k+1}}{\Delta x}$$

$$\begin{aligned} \bar{b}_{i,i} &= 1 + \frac{\Delta t}{\Delta x A_{w,i}^k} \left(K_{i-1}^{k+1} \frac{\bar{A}_{w,i-1/2}^{k+1} + K_i^{k+1} \bar{A}_{w,i+1/2}^{k+1}}{\Delta x} \right), \\ \bar{b}_{i,i+1} &= -\frac{\Delta t}{\Delta x A_{w,i}^k} \frac{K_i^{k+1} \bar{A}_{w,i+1/2}^{k+1}}{\Delta x} \\ \bar{c}_{i,1} &= \frac{\Delta t}{\Delta x T_{w,i}^k}, \quad i = 1, \quad \bar{c}_{i,2} = -\frac{\Delta t}{\Delta x T_{w,i}^k}, \quad i = l \\ \bar{d}_{\eta,i} &= \frac{\Delta t}{\Delta x T_{w,i}^k} \left(-A_{w,i}^k r u_{i+1/2}^k + q_{l,i}^{k+1} \right), \quad i = 1, \\ d_{\eta,i} &= \frac{\Delta t}{\Delta x T_{w,i}^k} \left(A_{w,i-1}^k r u_{i-1/2}^k + q_{l,i}^{k+1} \right), \quad i = l \\ d_{\eta,i} &= \frac{\Delta t}{\Delta x T_{w,i}^k} \left(A_{w,i-1}^k r u_{i-1/2}^k - A_{w,i}^k r u_{i+1/2}^k + q_{l,i}^{k+1} \right), \quad i = 2, 3, \dots, l-1 \\ d_{c,i} &= \frac{\Delta t}{\Delta x A_{w,i}^k} \left[\frac{K_{in}^{k+1} A_{w,i}^{k+1}}{\Delta x} \left(c_{in}^{k+1} - c^* \right) + q_{l,i}^{k+1} \left(c_{l,i}^{k+1} - c_i^k \right) \right. \\ &\quad \left. + Q_{i+1/2}^{k+1} c_i^k - Q_{i+1/2}^{k+1} * c_{i+1/2}^{k+1} \right], \quad i = 1 \end{aligned}$$

$$= I_{2l,2l} \begin{bmatrix} e_{\eta,i,1}^k \\ e_{\eta,i,2}^k \\ \vdots \\ e_{\eta,i,l}^k \\ \hline e_{c,i,1}^k \\ e_{c,i,2}^k \\ \vdots \\ e_{c,i,l}^k \end{bmatrix} + \begin{bmatrix} \bar{c}_{1,1} & 0 \\ 0 & 0 \\ \vdots & \vdots \\ 0 & 0 \\ \hline \bar{d}_{1,1} & 0 \\ 0 & 0 \\ \vdots & \vdots \\ 0 & 0 \\ \hline 0 & \bar{d}_{l,2} \end{bmatrix} \begin{bmatrix} Q_{c,1}^{k+1} \\ Q_{c,2}^{k+1} \end{bmatrix} + I_{2l,2l} \begin{bmatrix} d_{\eta,i,1}^k \\ d_{\eta,i,2}^k \\ \vdots \\ d_{\eta,i,l}^k \\ \hline d_{c,i,1}^k \\ d_{c,i,2}^k \\ \vdots \\ d_{c,i,l}^k \end{bmatrix}$$

$$\begin{aligned} d_{c,i} &= \frac{\Delta t}{\Delta x A_{w,i}^k} \left[q_{l,i}^{k+1} \left(c_{l,i}^{k+1} - c_i^k \right) + \left(Q_{i+1/2}^{k+1} - Q_{i-1/2}^{k+1} \right) c_i^k \right. \\ &\quad \left. - \left(Q_{i+1/2}^{k+1} * c_{i+1/2}^{k+1} - Q_{i-1/2}^{k+1} * c_{i-1/2}^{k+1} \right) \right], \quad i = 2, 3, \dots, l-1 \\ d_{c,i} &= \frac{\Delta t}{\Delta x A_{w,i}^k} \left[q_{l,i}^{k+1} \left(c_{l,i}^{k+1} - c_i^k \right) - Q_{i-1/2}^{k+1} c_i^k + Q_{i-1/2}^{k+1} * c_{i-1/2}^{k+1} \right], \quad i = l \end{aligned}$$

where $* c_{i+1/2}^{k+1} = \{ c_{i+1/2}^{k+1} (Q_{i+1/2}^{k+1} \geq 0) c_{i+1/2}^{k+1} (Q_{i+1/2}^{k+1} < 0) \}$, where c^* is the concentration target value, K_{in} and c_{in} are the dispersion coefficient and concentration of the incoming water. Note that c_{in} uses the outflow concentration of the upstream reach if the reach under concern is not the first one. All the variables at time step $k+1$ in the above matrices are calculated through a ‘forward estimation’ procedure.

$$f u_{i+1/2}^k = \frac{g \Delta t}{\Delta x \left(1 + g \frac{|v_{i+1/2}^k|}{C_z^2 R} \right)}, \quad r u_{i+1/2}^k = \frac{-A_{w,i+1/2}^k \left(\frac{Q_{i+1}^k * v_{i+1}^k - Q_i^{k*} v_i^k}{\Delta x} + v_{i+1/2}^k \frac{Q_{i+1}^k - Q_i^k}{\Delta x} \right) + v_{i+1/2}^k}{\left(1 + g \frac{|v_{i+1/2}^k|}{C_z^2 R} \right)}$$

where $\bar{Q}_i^k = (Q_{i+1/2}^k - Q_{i-1/2}^k)/2$, $\bar{A}_{w,i+1/2}^k = (A_{w,i+1}^k - A_{w,i}^k)/2$, ${}^*v_i^k = \{v_{i-1/2}^k (\bar{Q}_i^k \geq 0) v_{i+1/2}^k (\bar{Q}_i^k < 0)$.

Appendix B. Reduced model verification using extrapolated scenario of lateral flows

In Section 4, the reduced model is verified using the interpolated scenario of lateral flows and it achieves good model accuracy.

However, it is also important to verify the model according scenario extrapolation. Table B.1 provides the verification scenario and Figs. B.1, B.2 and B.3 show the reduced model accuracy using the extrapolated scenario.

Table B.1

Lateral flow scenario for reduced model verification (step changes happen between 5 and 8 h of the simulation).

Reach	Lateral 1		Lateral 2		Lateral 3	
	Discharge (m ³ /s)	Concentration (kg/m ³)	Discharge (m ³ /s)	Concentration (kg/m ³)	Discharge (m ³ /s)	Concentration (kg/m ³)
1	0.02 to 0.10	1.0 to 1.8	0.03 to 0.11	1.2 to 2.0	No third lateral	
2	0.02 to 0.10	1.2 to 2.0	0.03 to 0.11	1.4 to 2.1	No third lateral	
3	0.04 to 0.12	0.9 to 1.7	0.02 to 0.10	1.5 to 2.3	0.03 to 0.11	1.8 to 2.6
4	0.02 to 0.10	1.5 to 2.3	0.04 to 0.12	1.0 to 1.8	No third lateral	

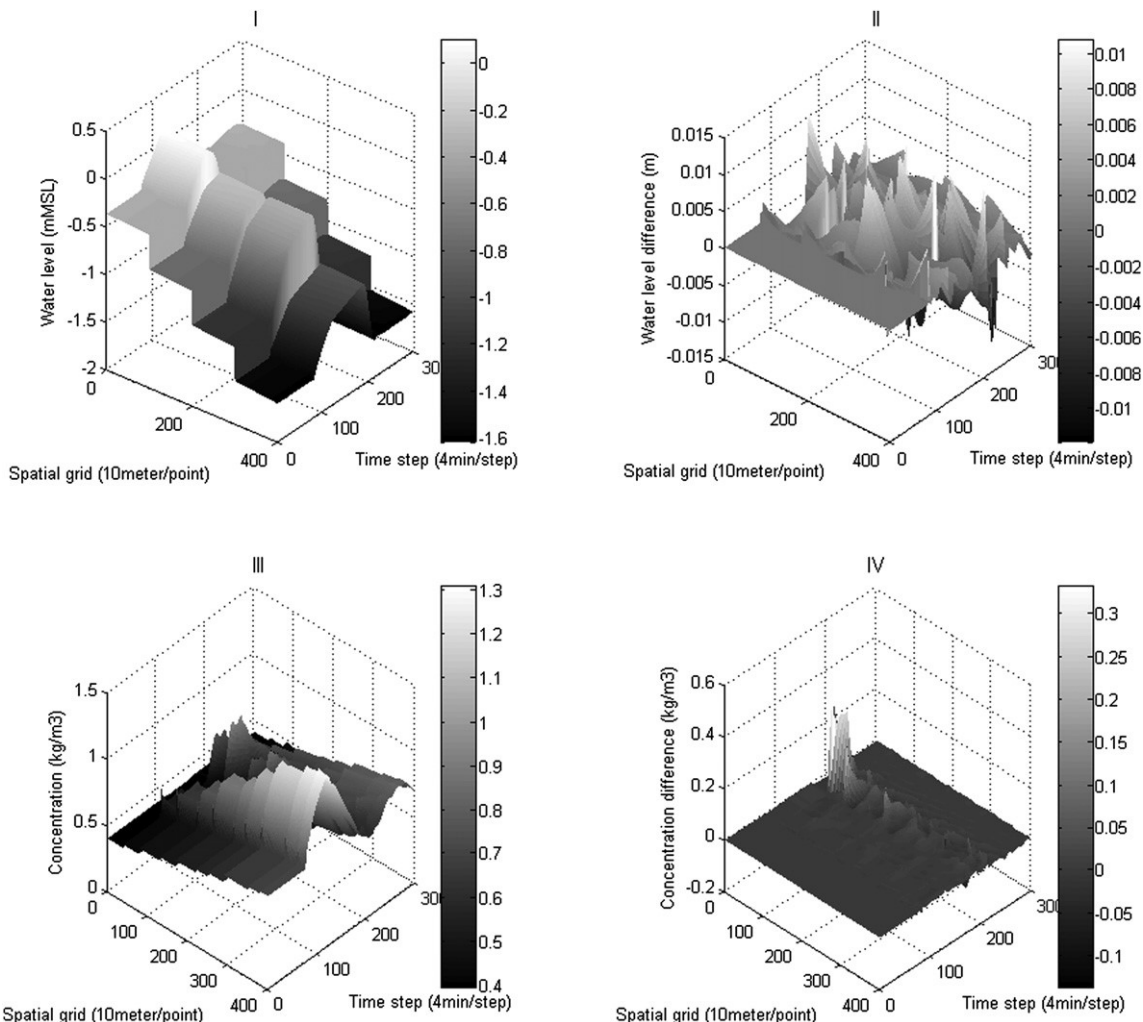


Fig. B.1. Reduced water level states (I) and concentration states (III) projected back to the original order, and the water level differences (II) and concentration differences (IV) between the reduced model and the original model.

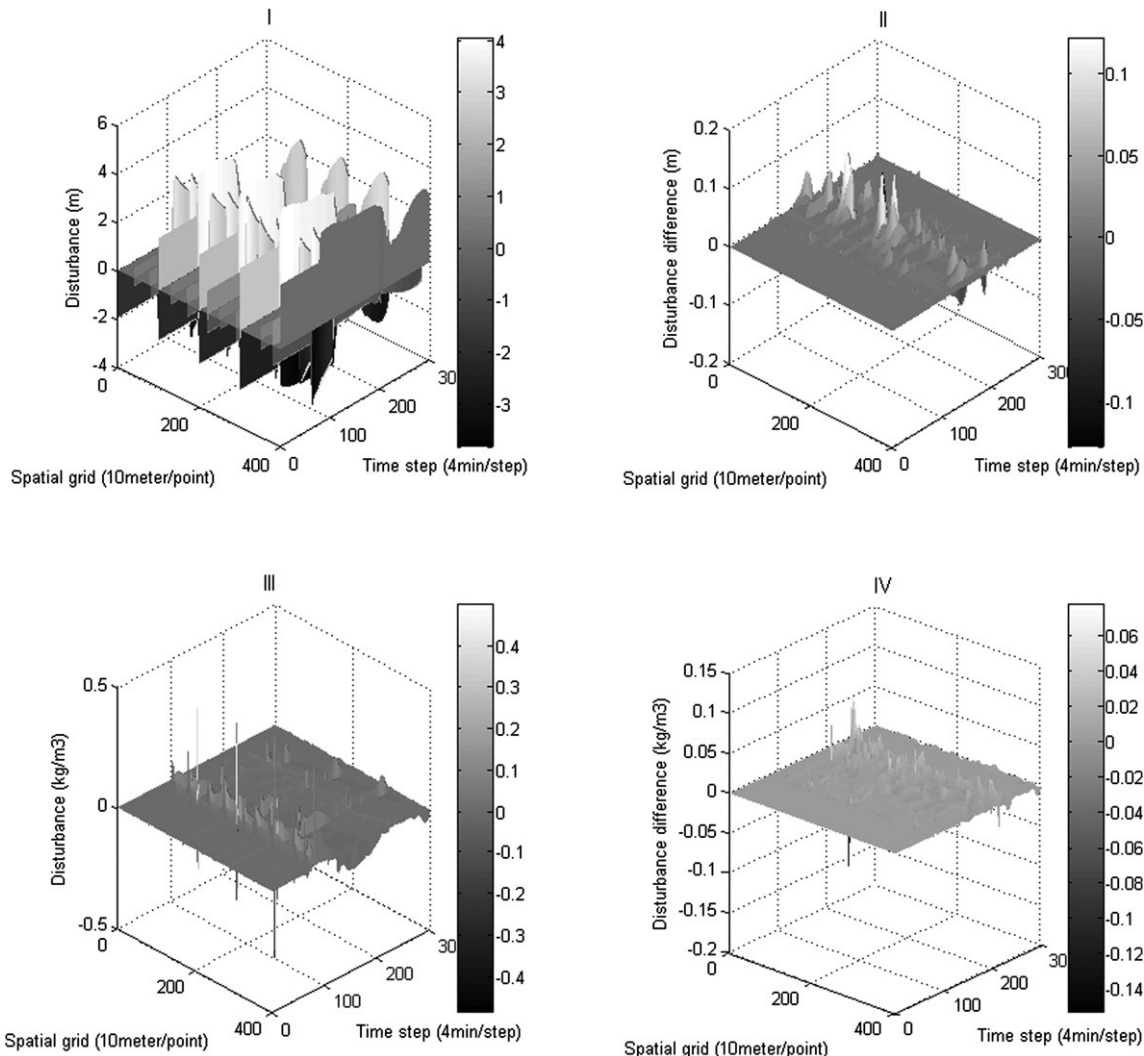


Fig. B.2. Reduced water quantity disturbances (I) and quality disturbances (III) projected back to the original order, and the water quantity disturbance differences (II) and water quality disturbance differences (IV) between the reduced model and the original model.

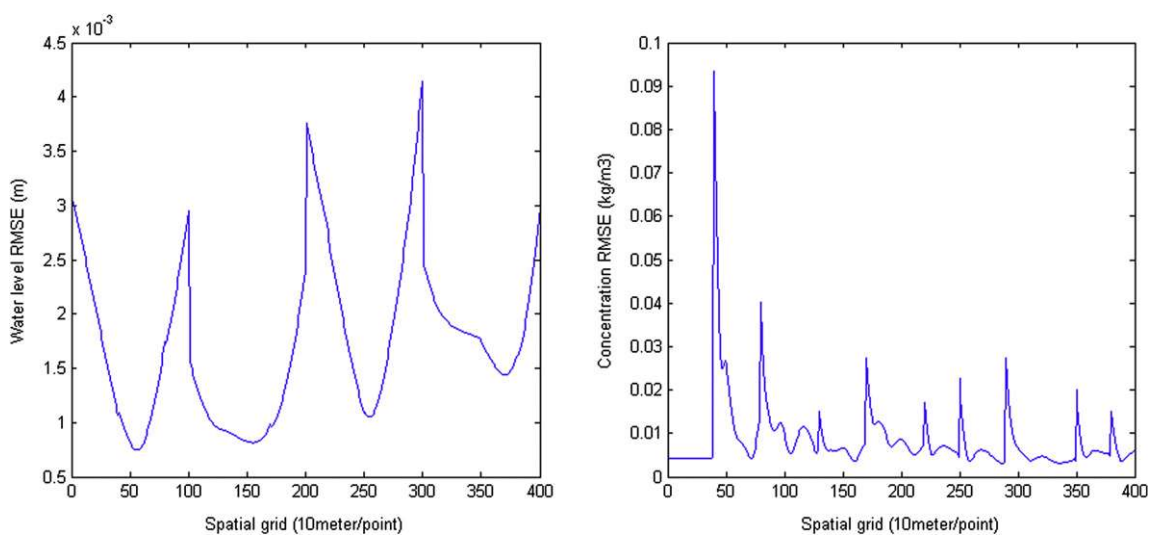


Fig. B.3. Root mean square error of the reduced model on water quantity and quality (extrapolated scenario).

References

- Augustijn, D.C.M., van den Berg, M., de Bruine, E., Korving, H., 2011. Dynamic control of salt intrusion in the Mark-Vliet river system, the Netherlands. *Water Resources Management* 25 (3), 1005–1020.
- Blanning, R.W., 1975. The construction and implementation of metamodels. *Simulation* 24 (6), 177–184.
- Borgonovo, E., Castaings, W., Tarantola, S., 2012. Model emulation and moment-independent sensitivity analysis: an application to environmental modelling. *Environmental Modelling & Software* 34, 105–115.
- Camacho, E.F., Bordons, C., 2004. *Model Predictive Control*, second ed. Springer-Verlag, New York.
- Castelletti, A., Galelli, S., Ratto, M., Soncini-Sessa, R., Young, P., 2012a. A general framework for Dynamic Emulation Modelling in environmental problems. *Environmental Modelling and Software* 34, 5–18.
- Castelletti, A., Galelli, S.R.M., Soncini-Sessa, R., 2012b. Data-driven dynamic emulation modelling for the optimal management of environmental systems. *Environmental Modelling and Software* 34, 30–43.
- Castelletti, A., Galelli, S., Restellia, M., and Soncini-Sessa, R., 2011. A data-driven Dynamic Emulation Modelling approach for the management of large, distributed water resources systems. In: 19th International Congress on Modelling and Simulation, Perth, Australia. December 12–16. 4008–4014.
- Chaves, P., Kojiri, T., 2007. Deriving reservoir operational strategies considering water quantity and quality objectives by stochastic fuzzy neural networks. *Advances in Water Resources* 30 (5), 1329–1341.
- Chaves, P., Tsukatani, T., Kojiri, T., 2004. Operation of storage reservoir for water quality by using optimization and artificial intelligence techniques. *Mathematics and Computers in Simulation* 67 (4), 419–432.
- Chen, G., Li, Y., Yan, G., 2010. A nonlinear POD reduced order model for limit cycle oscillation prediction. *Science China Physics, Mechanics & Astronomy*, Springer 53 (7), 1325–1332.
- Chow, V.T., 1959. *Open-channel Hydraulics*. McGraw-Hill, New York.
- Dhar, A., Datta, B., 2008. Optimal operation of reservoirs for downstream water quality control using linked simulation optimization. *Hydrological Processes* 22 (6), 842–853.
- Falcone, P., Borrelli, F., Tseng, H.E., Asgari, J., Hrovat, D., 2008. Linear time-varying model predictive control and its application to active steering systems. *International Journal of Robust and Nonlinear Control* 18 (8), 862–875.
- Fischer, H.B., 1979. *Mixing in Inland and Coastal Waters*. Academic Press, New York.
- Glasgow, H.B., Burkholder, J.A.M., Reed, R.E., Lewitus, A.J., Kleinman, J.E., 2004. Real-time remote monitoring of water quality: a review of current applications, and advancements in sensor, telemetry, and computing technologies. *Journal of Experimental Marine Biology and Ecology* 300 (1), 409–448.
- Ha, D.M., Lim, K.M., Khoo, B.C., Willcox, K., 2007. Real-time optimization using proper orthogonal decomposition: free surface shape prediction due to underwater bubble dynamics. *Computers & Fluids* 36 (3), 499–512.
- Ha, D.M., Tkalich, P., Chan, E.S., 2008. Tsunami forecasting using proper orthogonal decomposition method. *Journal of Geophysical Research-Oceans* 113, C06019.
- Hinze, M., Volkwein, S., 2005. Proper orthogonal decomposition surrogate models for nonlinear dynamical systems: error estimates and suboptimal control. *Dimension Reduction of Large-Scale Systems*, Springer 45, 261–306.
- Holmes, P., Lumley, J.L., Berkooz, G., 1998. *Turbulence, Coherent Structures, Dynamical Systems and Symmetry*. Cambridge University Press, Cambridge.
- Kerachian, R., Karamouz, M., 2007. A stochastic conflict resolution model for water quality management in reservoir-river systems. *Advances in Water Resources* 30 (4), 866–882.
- Lee, J.H., Lee, K.S., Kim, W.C., 2000. Model-based iterative learning control with a quadratic criterion for time-varying linear systems. *Automatica* 36 (5), 641–657.
- Leigh, J.R., 2004. *Control Theory*, second ed. the Institution of Engineering and Technology, London, United Kingdom.
- Liang, Y.C., Lee, H.P., Lim, S.P., Lin, W.Z., Lee, K.H., Wu, C.G., 2002. Proper orthogonal decomposition and its applications - part I: theory. *Journal of Sound and Vibration* 252 (3), 527–544.
- Litrico, X., Belaud, G., Fovet, O., 2011. Adaptive control of algae detachment in regulated canal networks. *IEEE International Conference on Networking, Sensing and Control (ICNSC)*, Delft, The Netherlands. April 11–13. 179–202.
- Litrico, X., Fromion, V., 2005. Design of structured multivariable controllers for irrigation canals. *44th IEEE Conference on Decision and Control*, the European Control Conference, Seville, Spain. December 12–15. 1881–1886.
- Marruedo, D.L., Alamo, T., Camacho, E.F., 2002. Input-to-state stable MPC for constrained discrete-time nonlinear systems with bounded additive uncertainties. *41st IEEE Conference on Decision and Control*, Las Vegas, Nevada, USA. December 10–13, 4619–4624.
- Mujumdar, P., Saxena, P., 2004. A stochastic dynamic programming model for stream water quality management. *Sadhana* 29 (5), 477–497.
- Negenborn, R.R., van Overloop, P.J., Keviczky, T., De Schutter, B., 2010. Distributed model predictive control for irrigation canals. *Networks and Heterogeneous Media* 4 (2), 359–380.
- Pannocchia, G., Rawlings, J.B., Wright, S.J., 2011a. Conditions under which suboptimal nonlinear MPC is inherently robust. *Systems & Control Letters* 60, 747–755.
- Pannocchia, G., Rawlings, J.B., Wright, S.J., 2011b. Inherently robust suboptimal nonlinear MPC: theory and application. *50th IEEE Conference on Decision and Control and European Control Conference (CDC-ECC)*, Orlando, FL, USA. December 12–15. 3398–3403.
- Pannocchia, G., Rawlings, J.B., Wright, S.J., 2011c. Is suboptimal nonlinear MPC inherently robust? *18th IFAC World Congress*, Milano, Italy. August 28–September 2, 7981–7986.
- Pannocchia, G., Wright, S.J., Rawlings, J.B., 2011d. Partial enumeration MPC: robust stability results and application to an unstable CSTR. *Journal of Process Control* 21 (10), 1459–1466.
- Ratto, M., Castelletti, A., Pagano, A., 2012. Emulation techniques for the reduction and sensitivity analysis of complex environmental models. *Environmental Modelling & Software* 34, 1–4.
- Ratto, M., Pagano, A., 2010. Using recursive algorithms for the efficient identification of smoothing spline ANOVA models. *Advances in Statistical Analysis* 94, 367–388.
- Ravindran, S.S., 2000. A reduced-order approach for optimal control of fluids using proper orthogonal decomposition. *International Journal for Numerical Methods in Fluids* 34 (5), 425–448.
- Razavi, S., Tolson, B.A., Burn, D.H., 2012. Numerical assessment of metamodeling strategies in computationally intensive optimization. *Environmental Modelling & Software* 34, 67–86.
- Schuurmans, J., 1997. Control of water levels in open-channels, PhD thesis, Delft University of Technology, The Netherlands. ISBN: 90-9010995-1.
- Schuurmans, J., Hof, A., Dijkstra, S., Bosgra, O.H., Brouwer, R., 1999. Simple water level controller for irrigation and drainage canals. *Journal of Irrigation and Drainage Engineering* 125 (4), 189–195.
- Shirangi, E., Kerachian, R., Bajestan, M.S., 2008. A simplified model for reservoir operation considering the water quality issues: application of the Young conflict resolution theory. *Environmental Monitoring and Assessment* 146 (1), 77–89.
- Siade, A.J., Putti, M., Yeh, W.W.G., 2010. Snapshot selection for groundwater model reduction using proper orthogonal decomposition. *Water Resources Research* 46 (8), W08539.
- Sirovich, L., 1987. Turbulence and the dynamics of coherent structures I: Coherent structures. II: Symmetries and transformations. III: Dynamics and scaling. *Quarterly Applied Mathematics* 45 (3), 561–590.
- Stelling, G.S., Duinmeijer, S.P.A., 2003. A staggered conservative scheme for every Froude number in rapidly varied shallow water flows. *International Journal for Numerical Methods in Fluids* 43 (12), 1329–1354.
- Thomann, R.V., Mueller, J.A., 1987. *Principles of Surface Water Quality Modeling and Control*. Harper & Row, Publishers, New York.
- van Overloop, P.J., Schuurmans, J., Brouwer, R., Burt, C.M., 2005. Multiple-model optimization of proportional integral controllers on canals. *Journal of Irrigation and Drainage Engineering* 131 (2), 190–196.
- van Overloop, P.J., 2006a. Model predictive control of canal systems in the Netherlands. *Irrigation and Drainage Systems* 20 (1), 90–109.
- van Overloop, P.J., 2006b. *Model Predictive Control on Open Water Systems*. IOS Press, Delft, The Netherlands.
- Wahlin, B.T., Clemmons, A.J., 2006. Automatic downstream water-level feedback control of branching canal networks: theory. *Journal of Irrigation and Drainage Engineering* 132 (3), 198–207.
- Winton, C., Pettway, J., Kelley, C., Howington, S., Eslinger, O.J., 2011. Application of Proper Orthogonal Decomposition (POD) to inverse problems in saturated groundwater flow. *Advances in Water Resources* 34 (12), 1519–1526.
- Xu, M., van Overloop, P.J., van de Giesen, N.C., Stelling, G.S., 2010a. Real-time control of combined surface water quantity and quality: polder flushing. *Water Science and Technology* 61 (4), 869–878.
- Xu, M., van Overloop, P.J., van de Giesen, N.C., 2010b. On the study of control effectiveness and computational efficiency of reduced Saint-Venant model in model predictive control. *Advances in Water Resources* 34 (2), 282–290.